drones

MDPI

Article

Optimization Methods for Unmanned eVTOL Approach Sequencing Considering Flight Priority and Traffic Flow Imbalance

Zhiqiang Wei [1], Xinlong Xiao [1,*], Xiangling Zhao [1] and Jie Yuan [2]

[1] College of Air Traffic Management, Civil Aviation University of China, Tianjin 300300, China; zqwei@cauc.edu.cn (Z.W.); xlzhao@cauc.edu.cn (X.Z.)
[2] School of Aeronautics, Northwestern Polytechnical University, Xi'an 710072, China; yuanjie2020@mail.nwpu.edu.cn
* Correspondence: 2023032041@cauc.edu.cn

Abstract: Approach sequencing is important for multiple unmanned electric vertical take-off and landing (eVTOL) vehicles landing in vertiport. In this study, the additional intermediate transition ring (AIR) approach procedure in a balanced traffic flow scenario, the single ring movement-allowed (SRMA) approach procedure in an imbalanced traffic flow scenario, and the additional ring and allowing of movement (ARAM) approach procedure in a mixed scenario are proposed and designed to improve the efficiency of approach sequencing. Furthermore, a priority loss classification method is proposed to consider the unmanned eVTOL flight priority difference. Finally, a multi-objective optimization model is constructed with the constraints of inflow, outflow, moment continuity, flow balance, and conflict avoidance. The objectives are minimizing the power consumption, total operation time, and priority loss. Comparison experiments are conducted, and the final results demonstrate that the ARAM approach procedure can reduce the average holding time by 8.4% and 7.6% less than the branch-queuing approach (BQA) and AIR in a balanced traffic flow scenario, respectively. The ARAM approach procedure can reduce the average holding time by 6.5% less than BQA in an imbalanced traffic flow scenario.

Keywords: advanced air mobility; unmanned electric vertical take-off and landing vehicle; approach sequencing; vertiport approach procedure; integer programming

check for updates

Academic Editor: Pablo Rodríguez-Gonzálvez

Received: 31 March 2025
Revised: 20 May 2025
Accepted: 21 May 2025
Published: 25 May 2025

Citation: Wei, Z.; Xiao, X.; Zhao, X.; Yuan, J. Optimization Methods for Unmanned eVTOL Approach Sequencing Considering Flight Priority and Traffic Flow Imbalance. *Drones* **2025**, *9*, 396. https://doi.org/10.3390/drones9060396

Copyright: © 2025 by the authors. Licensee MDPI, Basel, Switzerland. This article is an open access article distributed under the terms and conditions of the Creative Commons Attribution (CC BY) license (https://creativecommons.org/licenses/by/4.0/).

1. Introduction

As a component of advanced air mobility (AAM), vertiport is the infrastructure that ensures the safe and efficient operation of unmanned electric vertical take-off and landing (eVTOL) vehicles [1]. It is an important problem in sequencing the unmanned eVTOL on the vertiport airside [2]. Considering the traffic flow imbalance and the unmanned eVTOL flight priority difference, it is also important to study how to improve the existing approach procedures to reduce the holding time and improve the efficiency of approach sequencing [3].

Approach sequencing in traditional civil aviation is based on the sequencing of fixed flight procedures, where many factors are considered. Related research, including Qiu et al. [4], constructed a flight sequencing optimization model that considered runway constraints, control operation rules, and delay consumption. Du et al. [5] proposed a data-driven method to address the problem of arrival sequencing, where the study considered the prediction of the estimated time of arrival (ETA). Xu et al. [6] proposed a weighted constrained position shift (W-CPS) to empower different aircraft. Zhang et al. [7] empowered

the aircraft according to their importance to the aircraft, and considered the constraints of position, safe separation, same air route, and arrival time window. In the above-mentioned research, the problem of aircraft sequence needs to consider factors such as their approach rules, aircraft priority, safety intervals, and occupancy, which should also be considered in the problem of unmanned eVTOL sequencing.

There is little research on approach sequencing models for eVTOLs [8–12]. Related research includes the following: Benmoussa et al. [9] developed a simulation model that allows for estimating the flight performance and analyzing the mission of a fixed-wing multi-rotor unmanned aerial vehicle (UAV) with a hybrid electric propulsion system (HEPS). Kleinbekman et al. [10] constructed a mixed integer linear programming model to minimize the operation time of a given set of unmanned eVTOLs with the constraints of time window, position, and conflict avoidance. Song et al. [11,12] designed an optimal arrival sequence model to minimize the delay time of the unmanned eVTOL approach sequencing. For current research on unmanned eVTOL approach sequencing, the objectives focus on the delay time. However, it should not only focus on operation time for unmanned eVTOL. Other optimization objectives, such as power consumption, should be considered. Moreover, the priority of aircraft is also important, which is not considered in current research. A priority classification method is needed.

Approach procedure is another influential factor for the efficiency of approach sequencing. Current literature has shown that the point merge approach procedure can reduce delays and increase the efficiency of aircraft operations [13–17]. Hong et al. [13] designed an integer programming model to minimize the total arrival time of aircraft. The results illustrated that the designed model in the point merge system can increase the efficiency of arrival sequencing. Errico et al. [14] provided a methodology to reduce fuel consumption and environmental emissions in the point merge system. This methodology in the point merge system saved considerable fuel with respect to conventional standard arrival routes. Hong et al. [15] proposed a new sequencing and scheduling algorithm for the point merge system based on mixed integer linear programming to minimize the total landing time and delay time. The results illustrated that the point merge system can help reduce the delay. Liang et al. [16] constructed an integer programming model to eliminate conflicts and reduce delays. The comparative experiments showed that the proposed model in the point merge system can help reduce the average delay of the conventional standard arrival procedure. Tian et al. [17] designed an optimization method for the point merge procedure to minimize flight time, fuel consumption, pollutant emission, and noise impact. The results showed that the proposed optimization method in the point merge system could help reduce the above-mentioned elements. From the above-mentioned research, the point merge approach procedure can reduce the delay time, fuel consumption, and conflict, which can increase the capacity and approach efficiency of the airport. Therefore, improving the approach procedure may also increase the efficiency of the approach sequencing of eVTOLs.

There is little current research on unmanned eVTOL approach sequencing. Related research focuses on the construction and sequencing methods of approach procedures. Pradeep et al. [18,19] proposed an operation concept for unmanned eVTOL aircraft arrivals. In this operation concept, the unmanned eVTOL will transition and hover after completing the cruise and finally land on the pad. However, the eVTOL sequencing issue is not considered in this operational concept. Kleinbekman [10] proposed an approach procedure with a variable descent angle (VDA). This procedure can help reduce the delay in arriving at eVTOL. However, this approach procedure requires high clearance conditions and does not solve the problem of eVTOL sequencing. Josh et al. [20,21] proposed a terminal arrival airspace design method and unmanned eVTOL sequence method. In this arrival airspace,

eVTOL will fly in a circle in the holding ring. This approach procedure is similar to the point merge system in civil aviation, but it is more difficult to determine the interval between circling unmanned eVTOLs. It will also generate unnecessary power consumption during unmanned eVTOL circling. Shao et al. [22] improve the approach procedure in reference 23 by adding a fixed approach and departure routes and rules. However, the above-mentioned problems were not solved. Song et al. [11,12,23] proposed a branch queuing approach (BQA) to sequence the eVTOL by fixing the approach paths in each direction. This approach makes it easier to determine approach intervals and take advantage of the hoverability of eVTOL to reduce power consumption. However, this approach procedure does not solve the problem of the reordering of eVTOLs. This approach procedure is greatly affected by the direction of the approach traffic flow. Therefore, it is necessary to design an approach procedure to solve the problem of an eVTOL sequence based on the approach priority in the scenario of imbalanced traffic flow.

The problems of the current unmanned eVTOL approach sequencing can be concluded as follows:

(1) The problem of unmanned eVTOL flight priority difference should be considered in the unmanned eVTOL flight approach sequencing. Unmanned eVTOL flights may have priority differences in normality, emergency urgency, and emergency status.
(2) The problem of traffic flow imbalance may influence the operation efficiency of unmanned eVTOL flight approach sequencing. The direction of traffic flow may change due to the weather, departure, and the closing of approach routes, which results in traffic flow imbalance.
(3) The limitation of the traditional approach sequencing model with the objective of total operation time. Power consumption, unmanned eVTOL flight priority difference, etc., also need to be considered when optimizing unmanned eVTOL approach sequencing.

To address these above issues, the main contributions of this paper are listed below:

(1) The additional intermediate ring (AIR) approach procedure and a priority loss classification method are proposed to solve the problem of unmanned eVTOL flight priority difference. Unlike the approach procedures of VDA [10,18,19], circling [20–22] and BQA [11,12,23] cannot resequence the unmanned eVTOLs. The AIR approach procedure is constructed to improve the sequencing approach efficiency of unmanned eVTOL according to the unmanned eVTOL flight priority. The priority loss classification method focuses on the battery status and mission urgency of the unmanned eVTOL.
(2) The single ring movement-allowed (SRMA) approach procedure is proposed, and an approach direction matrix is constructed to solve the problem of unmanned eVTOL approach sequencing in an imbalanced traffic flow scenario. To solve the problem of traffic flow congestion in the approach procedure of BQA [11,12,23], the SRMA approach procedure is designed to alleviate the congestion of traffic flow imbalance and improve the approach sequencing based on unmanned eVTOL flight priority difference. The approach direction matrix is constructed to describe the traffic flow and approach procedure selection.
(3) A multi-objective optimization model is constructed to optimize the total operation time, power consumption, and priority loss of unmanned eVTOL. The optimization models only optimize the total operation time [10–12]. The multi-objective optimization model is constructed by 0-1 integer programming. This model considers the constraints of inflow, outflow, moment continuity, flow balance, and conflict avoidance with minimum power consumption, operation time, and priority loss.

The technology roadmap for this paper is shown in Figure 1. The current approach procedures include the VDA [10,18,19], circling [20–22], and the BQA [11,12,23]. A technical

comparison of the approach procedures proposed in this study is shown in Table 1. In Table 1, the AIR, SRMA, and ARAM approach procedures not only take advantage of the hoverability of unmanned eVTOL but also consider the resequencing method based on priority and traffic flow adjustment measures in the scenario of traffic flow imbalance.

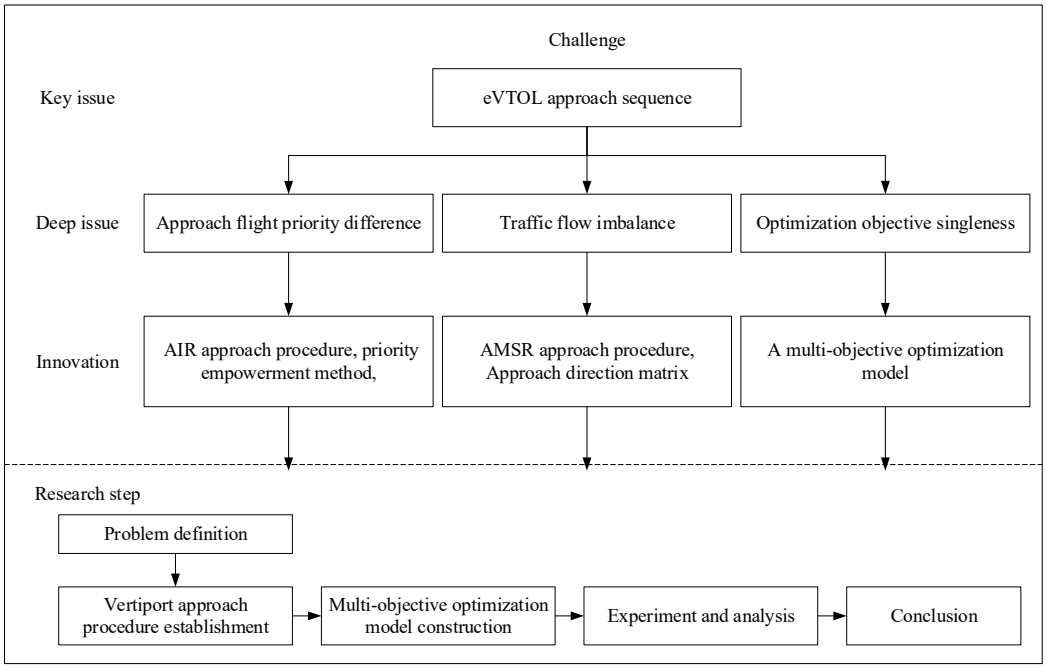


Figure 1. Technology roadmap.

Table 1. Technical comparison.

Approach Procedure	Advantages	Disadvantage	Applicable Environment
Traditional approach procedure of civil aviation			
VDA [10,18,19]	A changeable descent angle can reduce approach time and power consumption.	Large airspace is needed when operating on a large scale. It is hard to sequence when operating on a large scale.	Small-scale unmanned eVTOL operation. All types of unmanned eVTOL.
The ring structure and circling approach procedure			
Circling [20–22]	Suitable for large-scale unmanned eVTOL approaching.	Unnecessary power consumption caused by circling.	Medium-scale unmanned eVTOL operation. Fixed-wing unmanned eVTOL.
The ring structure and holding point approach procedure			
BQA [11,12,23]	Take advantage of the hoverability of unmanned eVTOL. Lower power consumption than circling.	Lack of resequence strategy based on unmanned eVTOL priority. Easily affected by traffic flow direction.	Large-scale unmanned eVTOL operation. All types of unmanned eVTOL.
AIR (This Paper)	Resequence strategy based on unmanned eVTOL priority.	Easily affected by traffic flow direction.	Large-scale unmanned eVTOL operation All types of unmanned eVTOL.
SRMA (This Paper)	Traffic flow adjustment strategy.	This may cause higher power consumption when resequencing unmanned eVTOL.	Large-scale unmanned eVTOL operation. All types of unmanned eVTOL.
ARAM (This Paper)	Resequence strategy based on unmanned eVTOL. Traffic flow adjustment strategy.		Large-scale unmanned eVTOL operation. All types of unmanned eVTOL.

The rest of this paper is organized as follows. Section 2 presents the problem of the vertiport approach sequencing and relevant assumptions. Section 3 describes the operation principle and design method of the proposed AIR, SRMA, and ARAM approach procedures. Section 4 focuses on the construction of the multi-objective optimization model. Section 5 presents validity experiments and compares the scenarios of balanced and imbalanced traffic flow. Section 6 concludes the results of the study.

2. Problem Definition

This study focuses on sequencing multiple unmanned eVTOLs during the approach phase, which begins at the end of the unmanned eVTOL cruise and ends with the unmanned eVTOL landing on the pad. The main objective of this study is to sequence the unmanned eVTOL considering the unmanned eVTOL flight priority difference, unmanned eVTOL total operation time, and eVTOL total power consumption.

To sequence the unmanned eVTOL and to ensure the unmanned eVTOL operation's safety, the unmanned eVTOL must approach based on the approach procedure. The general concept [24] of the unmanned eVTOL approach procedure is shown in Figure 2. The approach phase is divided into three parts: the initial approach phase, from the initial entry point to the intermediate point; the intermediate approach phase, from the intermediate point to the final entry point; and the landing phase, from the final entry point to the landing pad. The intermediate approach phase is divided into two parts. The first part is from the intermediate point to the MAP, and the second is from the MAP to the final entry point.

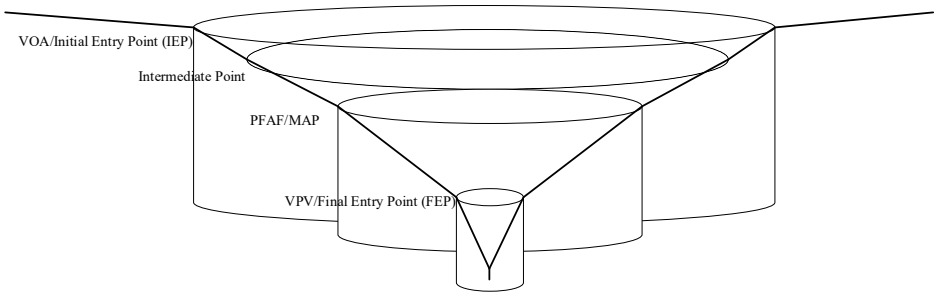


Figure 2. Vertiport approach procedure concept.

Based on the description of the approach procedure concept, the approach procedure can be simplified into several holding rings, as shown in Figure 3. The height and radius tuples of each ring are (h_0, r_0), (h_1, r_1), (h_2, r_2), . . ., (h_n, r_n), respectively. Subscript n is the number of holding rings.

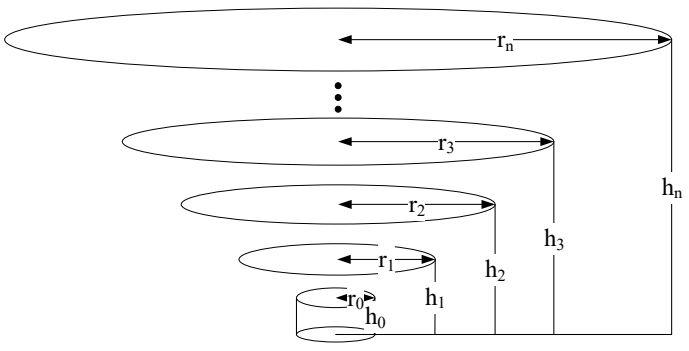


Figure 3. Vertiport airside holding ring.

There are holding points on the holding ring that make up the unmanned eVTOL approach procedure, as shown in Figure 4 [3]. For example, in Figure 4, the unmanned

eVTOL first flies from the holding point p_n through several holding rings to the holding point p_3, then flies to the holding point p_2, then flies from the holding point p_2 to the holding point p_1, and finally lands at p_0.

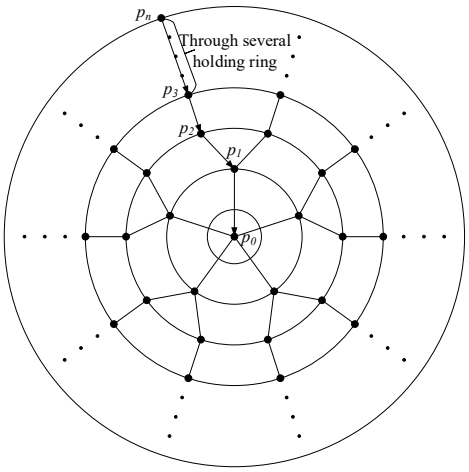


Figure 4. Vertiport approach procedure.

To further clarify the problem, the following operational assumptions are made:

(1) The scenario is assumed to be in an urban low-altitude airspace because the operation environment of unmanned eVTOL is an urban low-altitude area.
(2) The airside of the vertiport has sufficient airspace to support this approach procedure, and obstacles are not taken into account in the approach progress.
(3) The communication data of unmanned eVTOL vehicles are unbiased and transferred in real time, and communication failures are not considered.
(4) The ground capacity means the maximum number of unmanned eVTOLs that vertiports can accommodate. Currently, there are no large-scale vertiports in actual operation, so ground capacity data is difficult to obtain. Therefore, it is assumed that the ground capacity of the vertiport is unlimited.
(5) The operation phase of an unmanned eVTOL can be divided into three parts: descend, hover, and level. The unit power consumption of an unmanned eVTOL vehicle is constant during the individual operating phase described above.
(6) During the unmanned eVTOL approach, considering the small changes in unmanned eVTOL speed and distance between adjacent holding points, the unmanned eVTOL vehicle has a constant travel time between adjacent holding points.

3. Proposed Approach Procedures and Completion Method

In this section, the AIR approach procedure is described in detail in a balanced traffic scenario. Then, the SRMA approach procedure is presented in an imbalanced traffic flow scenario. Next, the additional ring and allowing of movement (ARAM) approach procedure is illustrated in the mixed scenario. Finally, the direction matrix is constructed to generate the traffic flow and select the approach procedure.

3.1. AIR Approach Procedure

For the problem of unmanned eVTOL approach sequencing based on unmanned eVTOL flight priority difference in a balanced traffic flow scenario, an intermediate transition holding ring is added in the vertiport approach procedure, which is depicted in red in Figure 5 and can be used as a transition route for unmanned eVTOL holding.

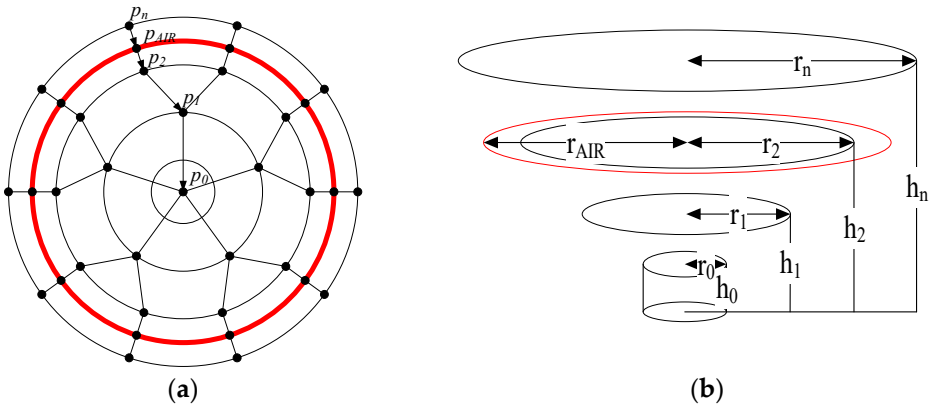


Figure 5. Vertiport AIR approach procedure. (**a**) Top view. (**b**) Corresponding side view.

For example, in Figure 5, the unmanned eVTOL vehicle first flies to the holding point p_n and then is selected to fly to either holding point p_{AIR} or holding point p_2. If it flies to holding point p_{AIR}, it should fly from holding point p_{AIR} to holding point p_2, then fly to holding point p_1, and finally land at p_0. This approach procedure is defined as the AIR approach procedure.

The unmanned eVTOL approach logic of AIR is illustrated in Figure 6. At time T_1, unmanned eVTOL vehicle Yellow (Y) arrives at the holding point p_n and is ready to descend towards the holding point p_{AIR}. Then, at time T_2, unmanned eVTOL vehicle Y arrives and is hovering at the holding point p_3. At the same time, unmanned eVTOL vehicle Cyan(C) arrives at the holding point p_n and is ready to descend towards the holding point p_2. At time T_3, unmanned eVTOL vehicle C is ready to descend, and unmanned eVTOL vehicle Y is hovering at the holding point p_{AIR}. At time T_4, unmanned eVTOL vehicle Y is levelling towards the holding point p_2, and has finished hovering. By implementing the above procedures, unmanned eVTOL vehicle C overtakes unmanned eVTOL vehicle Y.

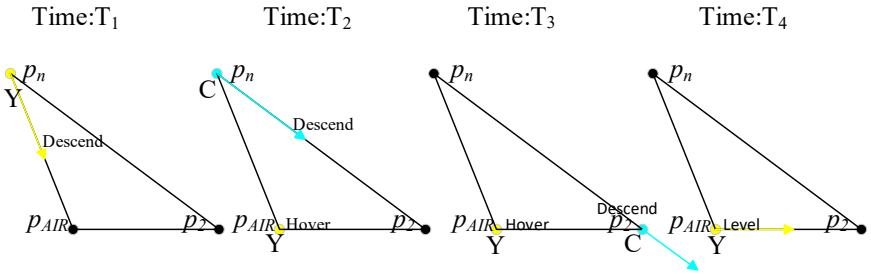


Figure 6. AIR approach procedure logic.

3.2. SRMA Approach Procedure

To solve the unmanned eVTOL flight priority difference problem in an imbalanced traffic flow scenario, the approach procedure is improved based on the vertiport approach procedure, which is shown in Figure 7 and is depicted in blue. The improved approach procedure allows unmanned eVTOL vehicles to move to other holding points in the same holding ring, making way for high-priority unmanned eVTOL vehicles in an imbalanced traffic flow scenario and relieving traffic flow congestion. This approach procedure is defined as the SRMA approach procedure.

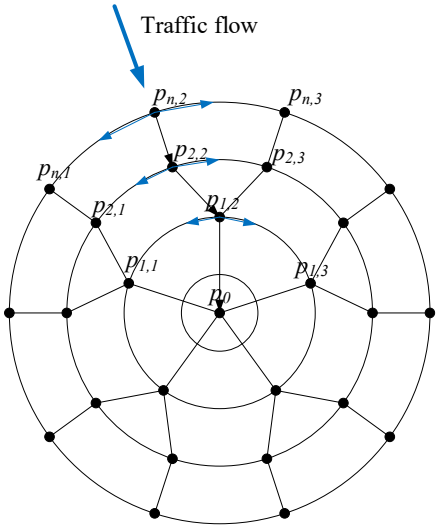


Figure 7. Vertiport SRMA approach procedure.

For example, in Figure 7, when an unmanned eVTOL vehicle arrives at holding point $p_{n,2}$, it can fly to $p_{n,2}$ or $p_{n,3}$ next. Similarly, when an unmanned eVTOL vehicle reaches $p_{2,2}$ or $p_{1,2}$, it can fly to $p_{2,1}$, $p_{2,3}$ or $p_{1,1}$, $p_{1,3}$ next. This approach procedure can confirm the optimal approach path in the direction of heavy traffic flow, thus making way for the high-priority unmanned eVTOL vehicles.

3.3. ARAM Approach Procedure

This section combines the improved approach procedure methods of AIR and SRMA to cope with the problem of the unmanned eVTOL flight priority difference in balanced and imbalanced traffic flow scenarios, which is the mixed scenario. As shown in Figure 8, the movement of the holding point is allowed in the same holding ring, and an intermediate transition holding ring is added in the vertiport approach procedure, defined as the ARAM approach procedure.

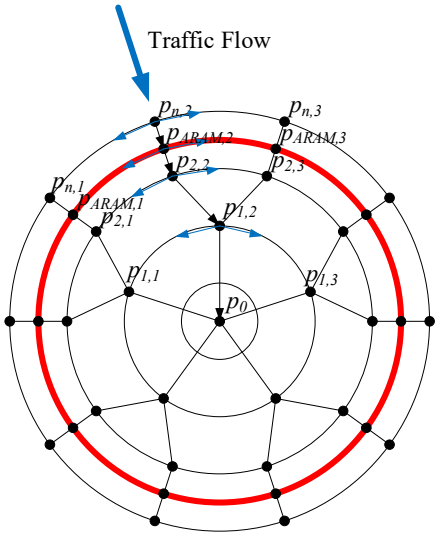


Figure 8. Vertiport ARAM approach procedure.

Unmanned eVTOL vehicles can fly to adjacent points below or in the same vicinity as the current altitude. For example, in Figure 8, when an unmanned eVTOL vehicle arrives at $p_{n,2}$, then it can fly to $p_{n,1}$ or $p_{n,3}$ or $p_{ARAM,2}$ or $p_{2,2}$. Similarly, if an unmanned eVTOL

vehicle arrives at $p_{ARAM,2}$, it can fly to $p_{ARAM,1}$ or $p_{ARAM,3}$ or $p_{2,2}$. Finally, an unmanned eVTOL vehicle lands at p_0.

3.4. Approach Procedure Selection Based on Direction Matrix

The unmanned eVTOL approach directions are divided into N_d parts. The unmanned eVTOL approach direction matrix is defined as $D = [D_1, \ldots, D_k, \ldots, D_{kmax}]$, where $D_k \in \{1, 2, \ldots, N_d\}$ represents the initial approach direction for unmanned eVTOL vehicle k ($k = 1, \ldots, k_{max}$).

Traffic flow imbalance is defined as the number of unmanned eVTOL vehicles approaching in a certain direction exceeding the total number of unmanned eVTOLs approaching by θ percent in a certain time period when a large number of eVTOLs arrive. The approach procedure selection flowchart is shown in Figure 9. The approach directions of unmanned eVTOLs are first randomly generated. Then, the approach directions are transformed into a direction matrix. Next, it is determined whether there is a traffic flow imbalance based on the direction matrix. If it is true, ARAM and SRMA approach procedures will be performed. If it is false, ARAM and AIR approach procedures will be performed.

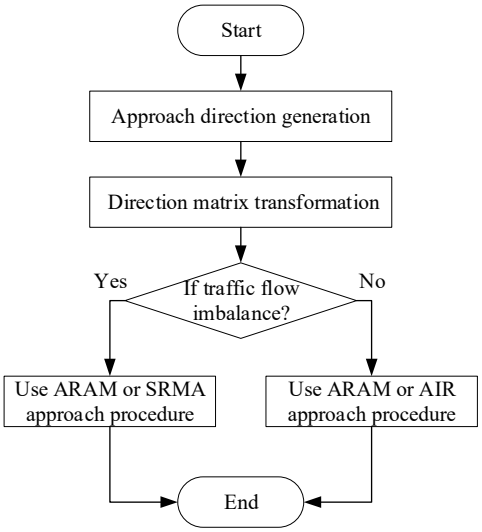


Figure 9. Approach procedure selection flowchart.

The example of the direction matrix is shown in Table 2. k represents the label of an unmanned eVTOL vehicle, and D_k represents the direction in which an unmanned eVTOL vehicle is approaching. For example, the initial approach direction of an unmanned eVTOL vehicle labelled 1 is 3, and the initial approach direction of an unmanned eVTOL vehicle labelled 2 is 4.

Table 2. Direction matrix example.

k	1	2	3	4	…	k_{max}
D_k	3	4	1	2	…	D_{kmax}

4. Optimization Model Construction

In this section, the multi-objective optimization model is constructed. The general model is given at first. Then, the details of the model are described.

The basic parameters are defined as follows:

(1) The set of departure points is $I = \{0, 1, 2, \ldots, I_{max}\}$;
(2) The set of arrival points is $J = \{1, 2, 3, \ldots, J_{max}\}$;
(3) The discrete time set is $T = \{0, 1, 2, \ldots, T_{max}\}$.

4.1. General Model

The general procedure model of the vertiport approach is constructed below:

$$Obj: z = Min(C_f \cdot \frac{F_{total}(x_{i,k,t})}{F_0} + C_t \cdot \frac{T_{total}(x_{i,k,t})}{T_0} + C_p \cdot \frac{L_p(x_{i,k,t})}{L_{p0}}) \quad (1)$$

$$A \cdot X \leq b \quad (2)$$

Equation (1) represents the objective function. The objective is to achieve the minimum power consumption, holding time, and priority loss. Where C_f, C_t, and C_p are the weights of unmanned eVTOL total power consumption, unmanned eVTOL total approach time, and unmanned eVTOL approach priority loss, respectively. F_0, T_0, and L_{p0} are the normalizing constants of total power consumption, total operation time, and priority loss, respectively. They are calculated from the optimal values under the single objective of total power consumption, total operation time, and priority loss, respectively. $F_{total}(x_{i,k,t})$, $T_{total}(x_{i,k,t})$, and $L_p(x_{i,k,t})$ represent unmanned eVTOL total power consumption, unmanned eVTOL total operation time, and unmanned eVTOL total priority loss, respectively, which are described in Section 4.3. $x_{i,k,t}$ is a decision variable, which is described in Section 4.2.

Equation (2) represents the constraints described in Section 4.4. X is a three-dimensional matrix consisting of decision variables $x_{i,k,t}$, A is a coefficient matrix, and b is a constant matrix.

In this model, each unmanned eVTOL has a cost per discrete time Δt. The priority loss means the total cost of all approaching unmanned eVTOLs. The details of the object and relative parameters are described in Section 4.3.

4.2. Decision Variables

The decision variable $x_{i,k,t}$ is an element of X, as defined in Equation (3) [25]. Where i is the holding point, k is the unmanned eVTOL label, and t is the time. For example, in Figure 10, $x_{p3,k3,t}$ refers to an unmanned eVTOL vehicle labelled k_3 at holding point p_3 at time t. An unmanned eVTOL vehicle has two states: flying (from one holding point to another holding point) and hovering (at a holding point).

$$x_{i,k,t} = \begin{cases} 1 & eVTOL\ k\ at\ i\ at\ time\ t \\ 0 & otherwise \end{cases} \quad (3)$$

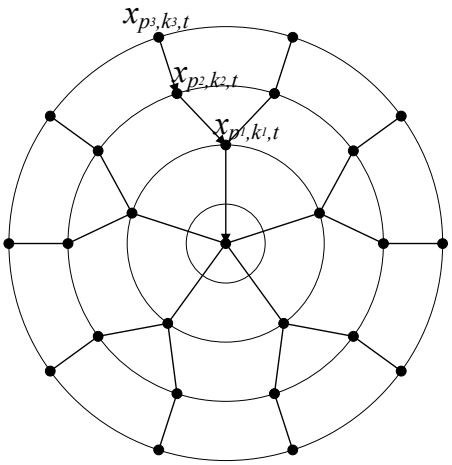


Figure 10. Three dimensions of decision variables.

4.3. Objective Function Description

This section addresses the problem of the unmanned eVTOL total power consumption calculation by summarizing unmanned eVTOL levelling, descending, and hovering power consumption. For the problem of unmanned eVTOL flight priority difference, a priority loss classification method is proposed by considering unmanned eVTOL battery status and mission urgency.

4.3.1. Total Power Consumption

Equations (4) and (5) calculate the total power consumption of eVTOL, where $F_{i,j}$ is the power consumption for movement between holding points, which includes the power consumption of descending, levelling, and hovering. $P_{i,j}$ is a time constant representing the moving time between holding point i and holding point j.

$$F_{total}(x_{i,k,t}) = \sum_{t\in T}\sum_{k\in K}\sum_{j\in J}\sum_{i\in I} F_{i,j}\cdot x_{i,k,t}\cdot x_{j,k,t+P_{i,j}} \tag{4}$$

$$F_{i,j} = \begin{cases} F_{hover} & if\ hold\ at\ i \\ F_{level} & if\ level\ from\ i\ to\ j \\ F_{descend} & f\ descend\ from\ i\ to\ j \end{cases} \tag{5}$$

$$F_{hover} = \sqrt{\frac{2(mg)^3}{N_R^3\rho\pi D_{R,i}^2}} \tag{6}$$

Equation (6) [26] is the calculation formula for eVTOL hover power consumption. Where m is the mass of the unmanned eVTOL, kg, g is the acceleration of gravity, m/s^2, N_R is the total number of propellers, pcs, ρ is the density of air, kg/m^3, and $D_{R,i}$ is the diameter of the propeller, m.

Equations (7) and (8) calculate the eVTOL power consumption of descending and levelling. The unmanned eVTOL descending power consumption should be less than the hovering power consumption. The unmanned eVTOL level power consumption should be higher than the hovering power consumption because the rotor is required to balance the weight of the unmanned eVTOL vehicle and propel the unmanned eVTOL vehicle in level flight.

$$F_{level} = (1+\alpha)\cdot F_{hover} \tag{7}$$

$$F_{descend} = (1-\beta)\cdot F_{hover} \tag{8}$$

α and β are constants, $\alpha > 0$ and $0 < \beta < 1$, which are dependent on the performance of unmanned eVTOL vehicle.

4.3.2. Priority Loss

Equation (9) represents the priority loss of the unmanned eVTOLs. C_k is a priority loss that considers the battery status and the mission urgency of unmanned eVTOL flights. The equation for C_k is given in Equation (10):

$$L_p(x_{i,k,t}) = \sum_{k\in K}\sum_{t\in T}\sum_{i\in I} C_k\cdot x_{i,k,t} \tag{9}$$

$$C_k = \varepsilon\cdot U_k + Q_k, (k\in K) \tag{10}$$

where U_k is the battery status priority loss for different unmanned eVTOL flights. Q_k is the mission urgency priority loss of different unmanned eVTOL flights, ε is a constant, and $0 < \varepsilon < 1$.

Q_k is divided into p types, as shown in Table 3. If the value of the mission urgency is high, the mission urgency priority loss Q_k is high.

$$SOC(t_{arrive} + \lambda \cdot t_{approach}) = SOC(t_{arrive}) - \frac{I_{current} \cdot (\lambda \cdot t_{approach})}{3600 \cdot BC} \quad (11)$$

Table 3. Mission urgency priority loss.

Category	1	2	3	4	...	p
Q_k	1	2	3	4	...	p

The battery status can be calculated by Equation (11) [27], where t_{arrive} is the arrival time of eVTOL, $t_{approach}$ is the required approach time without congestion, $SOC(t)$ is the remaining power of eVTOL at time t, λ is a constant to determine the minimum approach time, $I_{current}$ is the current, and BC is the battery capacity of eVTOL.

The categories of U_k are divided into q based on Equation (11). If the battery status is healthy, the power consumption priority is low. The step size of the battery status priority loss should be higher than the mission urgency priority loss. The step size is $p{\cdot}\varepsilon$. An example is shown in Table 4.

Table 4. Battery status priority loss.

Category	1	2	3	4	...	q
U_k	$p{\cdot}\varepsilon$	$2{\cdot}p{\cdot}\varepsilon$	$3{\cdot}p{\cdot}\varepsilon$	$4{\cdot}p{\cdot}\varepsilon$	...	$q{\cdot}p{\cdot}\varepsilon$

4.3.3. Total Operation Time

Equation (12) represents the total operation time of the unmanned eVTOL approach, and Δt represents the time step in this model.

$$T_{total}(x_{i,k,t}) = \sum_{i \in I} \sum_{j \in J} \sum_{k \in K} \sum_{t \in T} \Delta t \cdot P_{i,j} \cdot x_{i,k,t} \cdot x_{i,k,t+P_{i,j}} \quad (12)$$

4.4. Constraints

In this section, five constraints of the model are described: the constraint of inflow, the constraint of outflow, the constraint of moment continuity, the constraint of flow balance, and the constraint of conflict avoidance.

4.4.1. Constraint of Inflow

The constraint of inflow is used to specify the approach direction and approach time of eVTOL. Therefore, the constraint equations are as follows:

$$x_{0,k,0} = 1, (k \in K) \quad (13)$$

$$\sum_{t \in T} x_{i,k,t} \geq 1, (i = D_k, k \in K) \quad (14)$$

$$\sum_{t \in T} x_{i,k,t} = 0, (i \in O, i \neq D_k, , k \in K) \quad (15)$$

$$x_{D_{k_1},k_1,t_1} + x_{D_{k_2},k_2,t_2} \leq 2 + \frac{t_2 - t_1}{M}, (k_1 \in K, k_2 \in K, k_1 < k_2, D_{k_1} = D_{k_2}, t_1 \in T, t_2 \in T) \quad (16)$$

Constraint (13) ensures all unmanned eVTOLs arrive at the starting point at time 0. The starting point represents the area outside the outer ring in Figure 10. Constraints (14) and (15) guarantee that the initial approach direction of unmanned eVTOL vehicle k is D_k. O is the holding point set of the outer ring. Constraint (16) indicates that if unmanned

eVTOL vehicles k_1 and k_2 have the same initial approach direction, unmanned eVTOL vehicles with a small label reach the outer ring first. M is an infinite number.

4.4.2. Constraint of Outflow

The constraint of outflow needs to consider the problem of pad occupancy. Therefore, the equations are constructed as follows:

$$\sum_{t \in T} x_{J_{\max},k,t} = 1, (k \in K) \tag{17}$$

$$x_{I_{\max},k_1,t_1} + \sum_{t_2=t_1}^{t_2=t_1+\frac{\Delta t_1}{\Delta t}} x_{J_{\max},k_2,t_2} \leq 1, (k_1 \in K, k_2 \in K, k_1 \neq k_2, t_1 \in T, t_1 + \Delta t_1 \leq T_{\max}) \tag{18}$$

Constraint (17) means that each unmanned eVTOL occupies a landing pad for one unit of discrete time. Constraint (18) specifies that two unmanned eVTOLs need to have a time interval of $\Delta t_1/\Delta t$ when landing. $\Delta t_1/\Delta t$ is the required landing time interval for safety between two unmanned eVTOL vehicles in this model. Δt_1 is the landing time interval for safety between two unmanned eVTOL vehicles, and Δt_1 is a multiple of Δt.

4.4.3. Constraint of Moment Continuity

The moment continuity constraint is required to represent the time continuity of an unmanned eVTOL vehicle moving between holding points. The relevant equations are as follows:

$$\sum_{i \in I/0} x_{i,k,t} \leq 1, (k \in K, t \in T) \tag{19}$$

$$x_{i,k,t} \leq x_{i,k,t+\frac{\Delta t_2}{\Delta t}} + \sum_{j \in (L_{i,j}=1)} x_{j,k,t+P_{i,j}}, (i \in I/0, k \in K, t \in T, t + \Delta t < T_{\max}) \tag{20}$$

Constraint (19) prohibits unmanned eVTOL vehicles from appearing at multiple holding points at the same time. Constraint (20) ensures time continuity. At time t, if unmanned eVTOL vehicle k is at holding point i, unmanned eVTOL vehicle k should hold at holding point i by moment $t+\Delta t_2/\Delta t$ or arrive at holding point j by moment $t + P_{i,j}$. Δt_2 represents the required minimal time interval for safety, and Δt_2 is a multiple of Δt.

$L_{i,j}$ is a constant, representing whether holding point i and holding point j are connected.

4.4.4. Constraint of Flow Balance

The flow balance constraint is used to keep the balance of inflow and outflow in the intermediate holding point. The relevant equations are as follows:

$$\sum_{t \in T} \sum_{k \in K} \Big(\sum_{j \in (L_{i,j}=1)} x_{j,k,t+P_{i,j}} \Big) \cdot x_{i,k,t} = K_{\max} \tag{21}$$

$$\sum_{t_1 \in T} \sum_{k \in K} \Big(\sum_{i_1 \in (L_{i_1,i}=1)} x_{i_1,k,t_1-P_{i_1,i}} \Big) \cdot x_{i,k,t_1} = \sum_{t_2 \in T} \sum_{k \in K} \Big(\sum_{j \in (L_{i,j}=1)} x_{j,k,t_2+P_{i,j}} \Big) \cdot x_{i,k,t_2} \tag{22}$$

$$\sum_{t \in T} \sum_{k \in K} \Big(\sum_{i_1 \in (L_{i_1,I\max}=1)} x_{i_1,k,t-P_{i_1,i}} \Big) \cdot x_{I_{\max},k,t} = K_{\max} \tag{23}$$

Constraint (21) means the inflow in the entering area must be equal to the total number of unmanned eVTOL vehicles. Constraint (22) means the inflow must be equal to the outflow at intermediate holding point i. Constraint (23) means the outflow in the landing point must be equal to the total number of unmanned eVTOLs.

4.4.5. Constraint of Conflict Avoidance

The constraint of conflict avoidance [28] is used to avoid conflict when multiple eVTOLs operate. The constraint equation is as follows:

$$\sum_{k \in K} x_{i,k,t} \leq 1, (i \in J, t \in T) \tag{24}$$

Constraint (24) restricts unmanned eVTOL vehicles from simultaneously arriving at the same holding point. The conflict avoidance example is shown in Figure 11. For example, unmanned eVTOL vehicle 1 occupied this node from moment 1 to 3. Unmanned eVTOL vehicle 2 occupied this node from moment 4 to 7. We use this constraint to separate the occupied time to avoid conflicts.

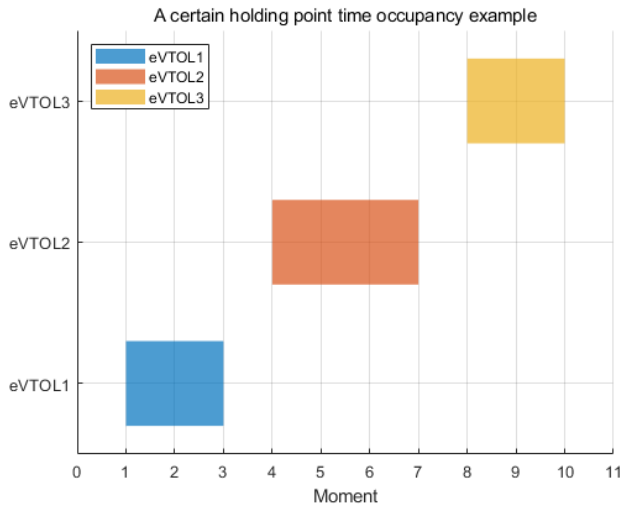


Figure 11. Conflict avoidance example.

5. Experiments and Analysis

In this section, the scenarios and relevant parameters are set first. Then, the evaluation method is presented. Next, typical unmanned eVTOL activities are analyzed as cases to verify the rationality of the proposed approach procedure. Finally, comparisons between the BQA (baseline) [11,12,23], AIR, SRMA, and ARAM approach procedures are made. The optimization model is solved by Python 3.7.12 + Gurobi 10.

5.1. Experiment Setup and Assumptions

The scenarios in this experiment are balanced and imbalanced traffic flow. In a balanced traffic flow scenario, the traffic flow is evenly distributed in all directions. In an imbalanced traffic flow scenario, the traffic flow is concentrated in several directions.

The parameters of unmanned eVTOL, approach procedure, and a multi-objective model are made. Due to the lack of actual vertiport airside design standards and safety interval standards between unknown eVTOLs, in addition to the known basic parameters of eVTOL, the remaining parameters will be assumed. The relevant parameters are set as follows:

5.1.1. Parameters of Unmanned eVTOL

The unmanned eVTOL parameters are shown in Table 5 [29].

Table 5. Unmanned eVTOL performance parameters.

Parameters	Autoflight Prosperity
m	1800 kg
N_R	10
$D_{R,i}$	3.14 m
α	0.1
β	0.05

The power consumption of unmanned eVTOL hovering, levelling, and descending can be calculated by Equations (6)–(8), as shown in Table 6.

Table 6. Unmanned eVTOL power consumption.

Parameters	Power Consumption
F_{hover}	29 kW·s
F_{level}	32 kW·s
$F_{descend}$	28 kW·s

5.1.2. Parameters of Vertiport Approach Procedure and Safety Interval Standard

The parameters of the approach procedure are shown in Table 7 [30].

Table 7. Parameters of approach procedure.

Parameters	Values
n	3
r_3	170 m
r_2	120 m
r_1	70 m
r_0	20
h_3	55 m
h_2	40 m
h_1	25 m
h_0	10
N_d	10

The discrete time step, the required minimal time interval and the required minimal landing time interval are set in Table 8.

Table 8. Related time parameters.

Parameters	Values
Δt	5 s
Δt_1	10 s
Δt_2	5 s

5.1.3. Parameters of Multi-Objective Optimization Model

The weight of each objective function is given in Table 9.

Table 9. Objective function weight.

Values	Weight
C_t	0.2
C_f	0.2
C_p	0.6

The ε is set to be 0.5 in this experiment. The parameters of the mission urgency and battery status are shown in Table 10.

Table 10. Mission urgency and battery status priority loss.

Parameters	Values	
Q_k	Cargo	1
	Passenger	2
U_k	Remaining high power	1
	Remaining low power	2

The category of priority loss can be calculated by Equation (9), which is shown in Table 11.

Table 11. Priority loss category.

Priority Category	High Priority	Next High Priority	Middle Priority	Low Priority
Battery status	Low	Low	High	High
Cargo or passenger	Passenger	Cargo	Passenger	Cargo
C_k	3	2.5	2	1.5

5.2. Evaluation Indicators

The indicators for evaluating and analyzing the experimental results of different approach procedures are defined as follows:

(1) Total power consumption F_{total} and average value $\overline{F}$

F_{total} represents the total power consumption of all unmanned eVTOLs, which is calculated by Equation (4). $\overline{F}$ represents the average power consumption of all unmanned eVTOLs. The equations $\overline{F}$ are displayed as follows:

$$\overline{F} = \frac{F_{total}}{K_{\max}} \tag{25}$$

(2) Average hovering time $\overline{HT}$

$\overline{HT}$ is defined to record the average holding time for all unmanned eVTOLs, which is presented as follows:

$$\overline{HT} = \frac{T_{total}}{K_{\max}} \tag{26}$$

(3) Priority loss of unmanned eVTOL flight L_p

The priority loss L_p is used to evaluate the priority sequencing of all unmanned eVTOL. The equation of L_p is described in Equation (9).

(4) Operating time (OT)

The total operating time (OT) is used to check the operating time of the last unmanned eVTOL vehicle in this system.

(5) Traffic flow pressure index (PI)

The traffic flow pressure index (PI) is used to test the traffic flow pressure used in the heavy traffic flow scenario. The equation is shown as follows:

$$PI = \frac{K_{above}}{K_{\max}} \tag{27}$$

K_{above} is the number of unmanned eVTOLs exceeding the average hovering time of all approach procedures.

The weights of F_{total}, $\overline{HT}$, and L_p are mentioned in Table 8. The weights of OT and PI are shown in Table 12.

Table 12. Indicator weight.

Indicators	Weight
C_o	*0.1*
C_{pi}	*0.1*

C_o represents the weight of the operation time, and C_{pi} is the weight of the traffic flow pressure index. The score of each approach procedure is calculated by Equation (28):

$$Score = \sum_{i \in Indicators} Score_i \cdot C_i \tag{28}$$

where $Score_i$ is the score of each indicator. C_i is the weight of each indicator. Higher scores indicate better results for the approach procedure.

5.3. Model and Approach Procedure Verification

In this section, the BQA procedure is compared as a baseline to validate the rationality of the proposed approach procedures. Twenty unmanned eVTOLs are set up to test the correctness of the approach procedure without approach priority in balanced and imbalanced traffic flow scenarios. The solution times of AIR, SRMA, and ARAM approach procedures are 20 s, 20 s, and 120 s. The computational complexity is O(n^3), and as the number of eVTOLs increases, the computational time increases exponentially. The solution comparison picture is shown in Figure 12. The strategy used is first-come-first-served, and the minimum holding time and power consumption are used as the objective function. If the approach procedure is correct, the holding time and power consumption distribution of different approach procedures should be similar.

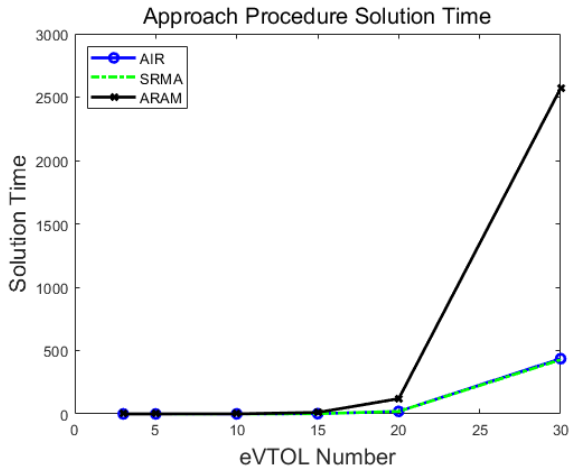
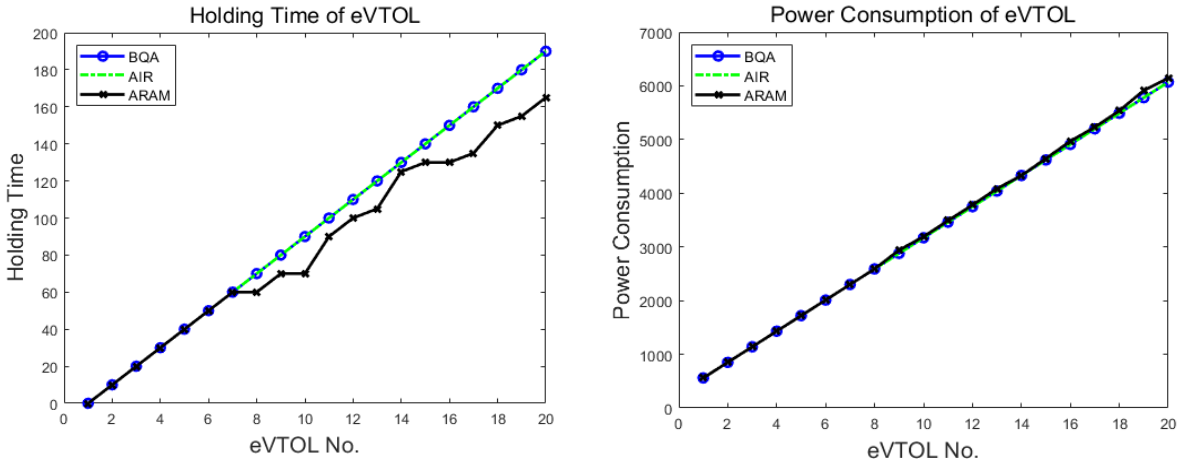


Figure 12. Approach procedure Solution Time.

The experiment results in a balanced traffic flow scenario, as shown in Table 13 and Figure 13. It is concluded that the AIR approach procedure and ARAM approach are almost the same as the BQA in the distributions of holding time and power consumption in a balanced traffic flow scenario without priority.

Table 13. Comparisons of BQA, AIR, and ARAM in a balanced traffic flow scenario without priority.

Approach Procedure	$\overline{F}$	$\overline{HT}$
BQA	3315 kW·s	95 s
AIR	3315 kW·s	95 s
ARAM	3342.8 kW·s	84.75 s



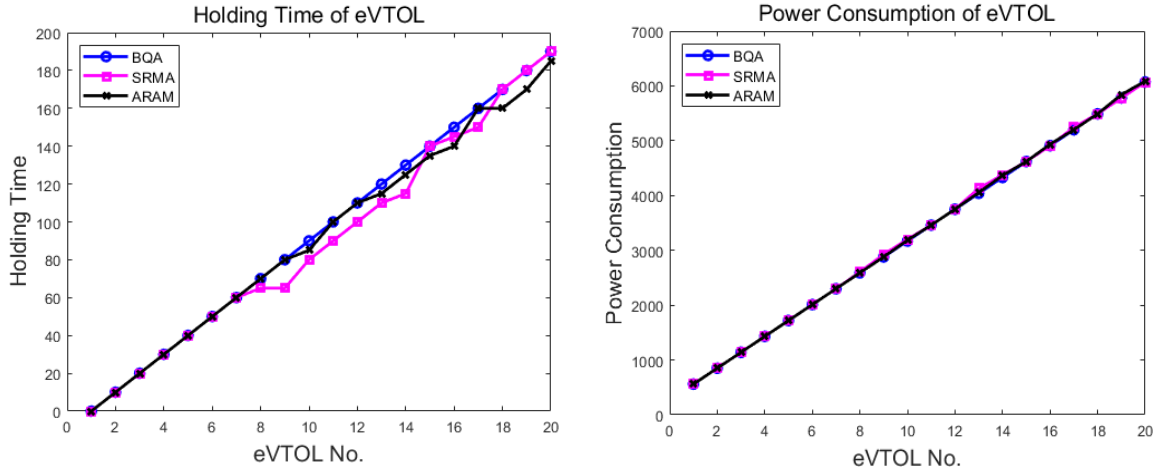
(**a**) Holding time line chart. (**b**) Power consumption line chart.

Figure 13. Line chart in balanced traffic flow scenario.

The SRMA and the ARAM approach procedures are also the same as the BQA procedure in the distributions of holding time and power consumptiown in an imbalanced traffic flow scenario without priority, which is shown in Table 14 and Figure 14.

Table 14. Comparisons of BQA, SRMA, and ARAM in an imbalanced traffic flow scenario without priority.

Approach Procedure	$\overline{F}$	$\overline{HT}$
BQA	3315 kW·s	95 s
SRMA	3328.5 kW·s	90.5 s
ARAM	3323.3 kW·s	92.5 s



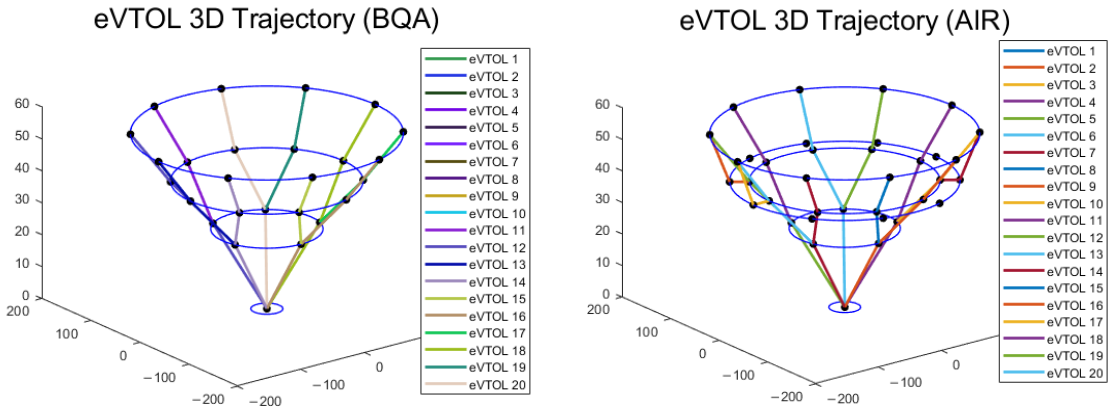
(**a**) Holding time line chart. (**b**) Power consumption line chart.

Figure 14. Line chart in imbalanced traffic flow scenario.

In summary, the experimental results of the proposed approach procedure are similar to the BQA in scenarios without priority, which can demonstrate the feasibility of the proposed approach procedures. However, their solution time is too long. This study focuses on the feasibility of the multi-objective model. A reduction in solution time requires further research in the future.

5.4. Analysis of Approach Priority Difference

In this section, 20 unmanned eVTOLs are set up in a balanced traffic flow scenario to compare between the BQA and AIR. The approach trajectories are shown in Figure 15.



(**a**) Approach trajectories of the BQA. (**b**) Approach trajectories of the AIR.

Figure 15. Approach trajectories (BQA and AIR).

The comparisons of the approach procedure between the BQA and AIR are shown in Table 15. The total power consumption of AIR is increased to 45 kW·s higher than the BQA. The average holding time of AIR is reduced to 0.75 s less than the BQA. The priority loss of AIR is reduced to 7 less than BQA. The operating time and the pressure index of AIR remain constant. The results show that the AIR approach procedure scores higher than the BQA approach procedure. Therefore, the AIR approach procedure is better regarding average holding time and priority sequencing.

Table 15. Comparison of indexes between BQA and AIR.

Approach Procedure	F_{total} (*Score*)	$\overline{HT}$ (*Score*)	L_p (*Score*)	*OT* (*Score*)	*P* (*Score*)	*Score*
BQA	66,300 kW·s (+1)	95 s *(+0)*	876 *(+0)*	210 s *(+0)*	0.5 *(+0)*	0.2
AIR	66,345 kW·s (+0)	94.25*s (+1)*	869 *(+1)*	210 s *(+0)*	0.5 *(+0)*	0.8

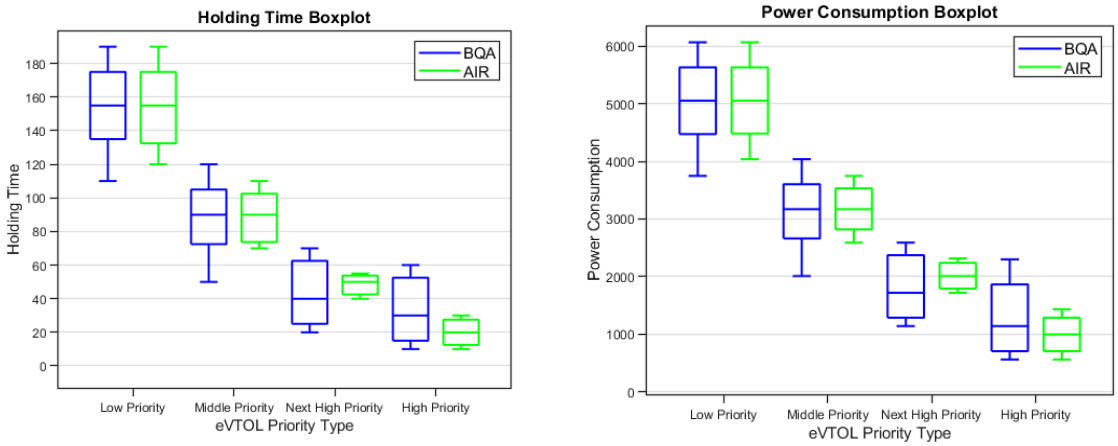
Tables 16 and 17 show the average power consumption and average holding time in different priorities. In the AIR approach procedure, the average power consumption of high-priority unmanned eVTOL vehicles is reduced by 290 kW·s compared to the BQA. The average holding time of high-priority unmanned eVTOLs is reduced to 10 s less than the BQA. The boxplots of holding time and power consumption are shown in Figure 16.

Table 16. Comparison of $\overline{F}$ between BQA and AIR with different priorities.

Approach Procedure	Low Priority	Middle Priority	Next High Priority	High Priority
BQA	5018.8 kW·s	3112 kW·s	1816.7 kW·s	1285 kW·s
AIR	5056.9 kW·s	3173 kW·s	2015 kW·s	995 kW·s

Table 17. Comparison of $\overline{HT}$ between BQA and AIR with different priorities.

Approach Procedure	Low Priority	Middle Priority	Next High Priority	High Priority
BQA	153.75 s	88 s	43.3 s	25 s
AIR	154.375 s	89 s	48.3 s	15 s



(**a**) Holding time boxplot. (**b**) Power consumption boxplot.

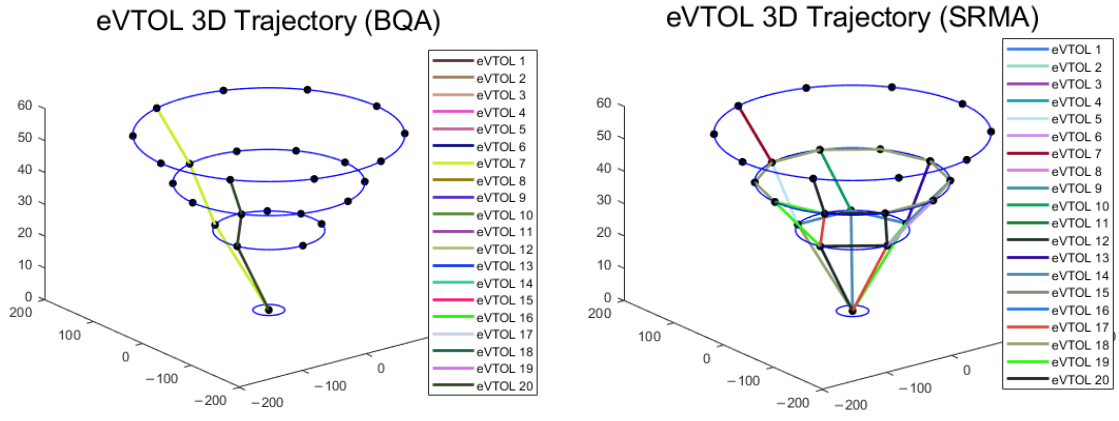
Figure 16. Holding time and power consumption distribution boxplot (BQA and AIR).

The distributions of power consumption and holding time in the high-priority unmanned eVTOLs show a downward concentration compared to the BQA approach procedure. Therefore, the AIR approach procedure is better than the BQA approach procedure in terms of average holding time and power consumption of high-priority flights.

In summary, the AIR approach procedure is better than the BQA in a balanced traffic flow scenario. The reason for these phenomena is that the intermediate transition holding ring can act as a holding area for low-priority unmanned eVTOLs, thus giving way to high-priority unmanned eVTOLs. As a result, it reduces the average power consumption and holding time of high-priority unmanned eVTOLs by 22.5% and 40%.

5.5. Analysis of Traffic Flow Imbalance

In this section, 20 unmanned eVTOLs are set in an imbalanced traffic flow scenario. The comparative approach trajectories are depicted in Figure 17. It can be seen that when the traffic flow is concentrated in a few directions, the airspace is used less than that in a balanced traffic flow scenario.



(**a**) Approach trajectories of the BQA. (**b**) Approach trajectories of the SRMA.

Figure 17. Approach trajectories (BQA and SRMA).

The comparisons of the approach procedure between the BQA and SRMA are shown in Table 18. The total power consumption of SRMA is increased to 2610 kW·s higher than the BQA. The average holding time of SRMA is reduced to 43.5 s less than the BQA. The priority loss of SRMA is reduced to 52 less than the BQA. The operating time of SRMA remains constant. The traffic flow pressure index of SRMA is reduced to 0.45 less than the BQA. The final score shows that the SRMA approach procedure has a higher score than the BQA.

Table 18. Comparison of indexes between BQA and SRMA.

Approach Procedure	F_{total} (*Score*)	$\overline{HT}$ (*Score*)	L_p (*Score*)	*OT* (*Score*)	*P* (*Score*)	*Score*
BQA	66,300 kW·s (+1)	95 s (+0)	972 (+0)	210 s (+0)	0.55 (+0)	0.2
SRMA	68,910 kW·s (+0)	51.5 s (+1)	920 (+1)	210 s (+0)	0.1 (+1)	0.9

Tables 19 and 20 illustrate the average power consumption and holding time in different priorities. In the SRMA approach procedure, the average power consumption of high-priority and next-high-priority unmanned eVTOL vehicles is reduced to 432.5 kW·s and 2255 kW·s less than the BQA. The average holding time of low-priority, middle-priority, next-high-priority, and high-priority unmanned eVTOL vehicles in SRMA is reduced to 45 s, 7 s, 101.6 s, and 42.5 s less than the BQA.

Table 19. Comparison of $\overline{F}$ between BQA and SRMA with different priorities.

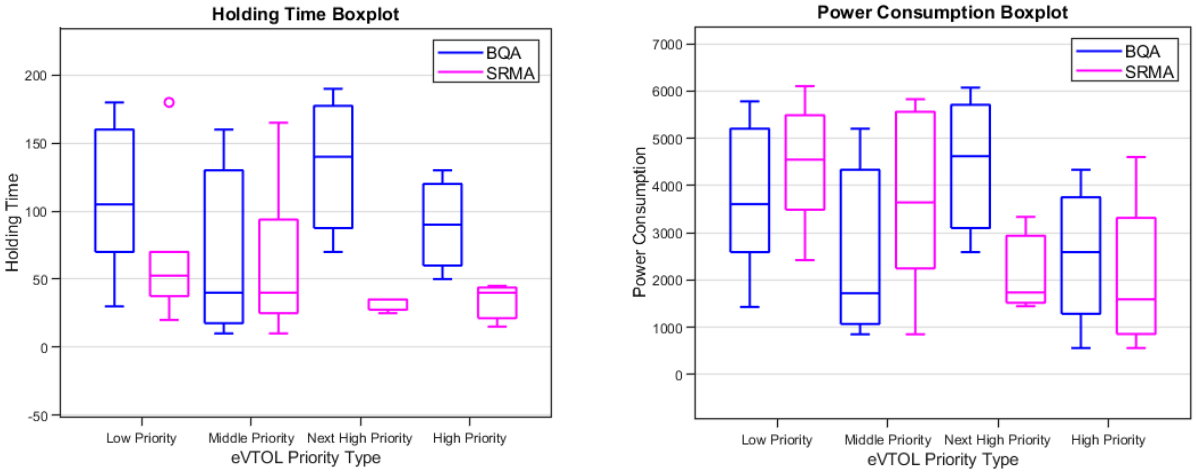
Approach Procedure	Low Priority	Next High Priority	High Priority
BQA	3750 kW·s	4426.7 kW·s	2517.5 kW·s
SRMA	4445 kW·s	2171.7 kW·s	2085 kW·s

Table 20. Comparison of $\overline{HT}$ between BQA and SRMA with different priorities.

Approach Procedure	Low Priority	Middle Priority	Next High Priority	High Priority
BQA	110 s	70 s	133.3 s	67.5 s
SRMA	65 s	63 s	31.7 s	25 s

The distributions of holding time and power consumption are shown in Figure 18. The distributions of holding time for all priority unmanned eVTOLs in SRMA present a downward concentration compared to the BQA. The power consumption of high-priority and next-high-priority unmanned eVTOLs in SRMA presents a downward concentration distribution compared to the BQA. Therefore, the SRMA approach is better for the priority sequencing of unmanned eVTOL vehicles.

In summary, the SRMA approach procedure can reduce the traffic flow pressure caused by traffic flow imbalance and increase the efficiency of approach sequencing based on priority because the SRMA approach procedure can also give way to high-priority unmanned eVTOLs. The SRMA approach procedure has a 45% reduction in average holding time despite a 3.9% increase in power consumption.

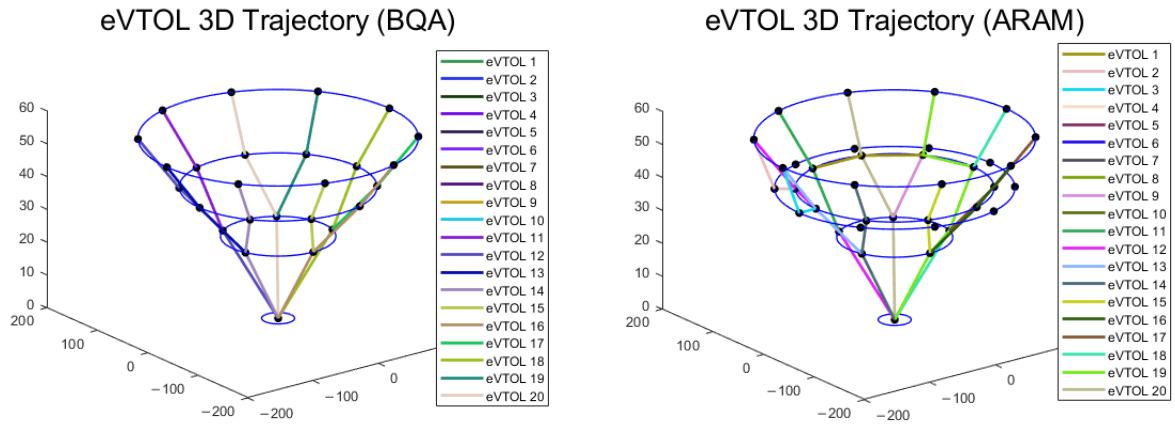


(**a**) Holding time boxplot. (**b**) Power consumption boxplot.

Figure 18. Holding time and power consumption comparison boxplots (BQA and SRMA).

5.6. Analysis of Comprehensive Scenario

In this section, the 20 unmanned eVTOLs are set up. The comparisons are made in balanced and imbalanced traffic flow scenarios. The unmanned eVTOL approach trajectories of balanced traffic flow are shown in Figure 19. The ARAM approach procedure is more complex and uses more airspace than the BQA procedure.



(**a**) Approach trajectories of the BQA. (**b**) Approach trajectories of ARAM.

Figure 19. Approach trajectories (balanced traffic flow).

The comparisons of the approach procedure between the BQA and AIR are shown in Table 21. The total power consumption of ARAM is increased by 240 kW·s more than the BQA and 195 kW·s more than AIR. The average holding time of AIR is reduced to 8 s less than the BQA and 7.25 s less than AIR. The priority loss of AIR is reduced to 5 less than the BQA and is the same as AIR. The operating time remains constant in the ARAM approach procedure. The pressure index is reduced to 0.05 less than the BQA and AIR. The ARAM approach procedure has a higher score than the other approach procedures. Therefore, the ARAM approach procedure can reduce the holding time and relieve the traffic flow pressure.

Table 21. Comparison of indexes between BQA, ARAM, and AIR.

Approach Procedure	F_{total} (*Score*)	$\overline{HT}$ (*Score*)	L_p (*Score*)	*OT* (*Score*)	*P* (*Score*)	*Score*
BQA	66,300 kW·s (+2)	95 s (+0)	876 (+0)	210 s (+0)	0.5 (+0)	0.4
ARAM	66,540 kW·s (+0)	87 s (+2)	869 (+1)	210 s (+0)	0.45 (+1)	1.1
AIR	66,345 kW·s (+1)	94.25 (+1)	869 (+1)	210 s (+0)	0.5 (+0)	1.0

Tables 22 and 23 display the average power consumption and holding time in different priorities. In the ARAM approach procedure, the average power consumption of high-priority unmanned eVTOL vehicles is reduced to 290 kW·s less than BQA. The average power consumption of low-priority, middle-priority, and next-high-priority vehicles in the ARAM approach procedure is increased to 11.2 kW·s, 18 kW·s, and 5 kW·s more than AIR. The average holding time of low-priority, middle-priority, and high-priority unmanned eVTOL vehicles in the ARAM approach procedure is reduced to 13.125 s, 6 s, and 10 s, respectively, less than in the BQA. The average holding time of low-priority, middle-priority, and next-high-priority unmanned eVTOL vehicles in the ARAM approach procedure is reduced to 13.75 s, 6 s, and 1.63 s, respectively, less than AIR.

Table 22. Comparison of $\overline{F}$ between BQA, ARAM, and AIR.

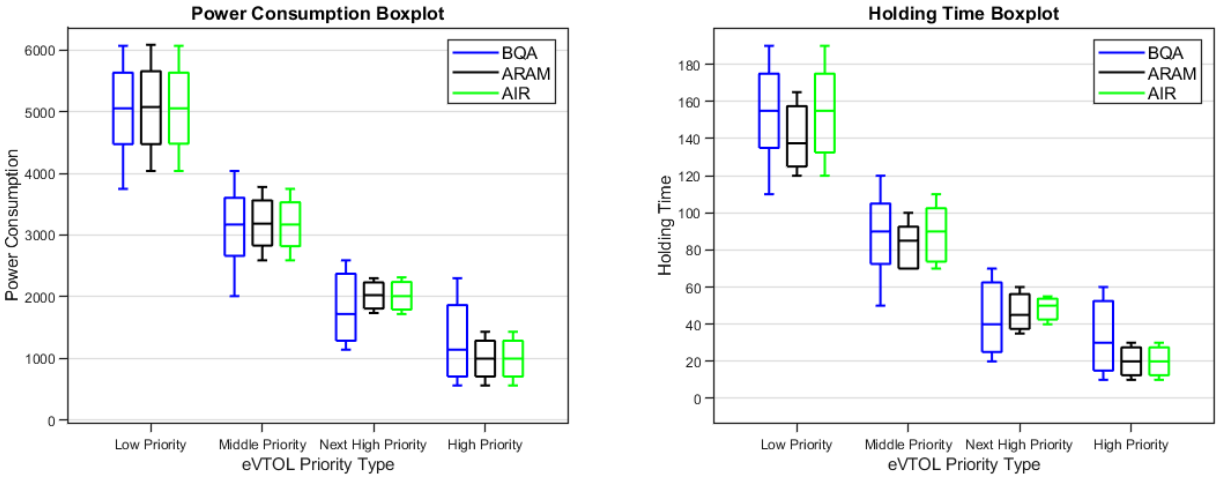
Approach Procedure	Low Priority	Middle Priority	Next High Priority	High Priority
BQA	5018.8 kW·s	3112 kW·s	1816.7 kW·s	1285 kW·s
ARAM	5068.1 kW·s	3191 kW·s	2020 kW·s	995 kW·s
AIR	5056.9 kW·s	3173 kW·s	2015 kW·s	995 kW·s

Table 23. Comparison of $\overline{HT}$ between BQA, ARAM, and AIR.

Approach Procedure	Low Priority	Middle Priority	Next High Priority	High Priority
BQA	153.75 s	88 s	43.3 s	25 s
ARAM	140.625 s	83 s	46.67 s	15 s
AIR	154.375 s	89 s	48.3 s	15 s

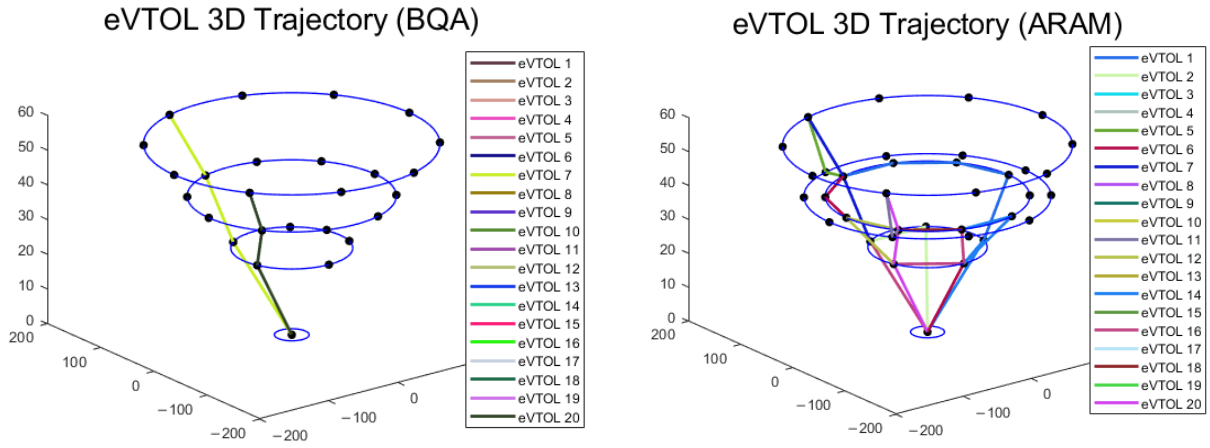
The distributions of holding time and power consumption are shown in Figure 20. The holding time of all priority unmanned eVTOLs in ARAM has a downward concentration distribution compared to other approach procedures. The power consumption of all priority unmanned eVTOLs is almost the same as that of AIR at the distribution level. The power consumption of high-priority unmanned eVTOLs presents a lower concentration distribution than that of the BQA.

The unmanned eVTOL approach trajectories are shown in Figure 21. The ARAM approach procedure can also disperse the traffic flow. The comparisons of the approach procedure between the BQA, ARAM, and SRMA are shown in Table 24. The total power consumption of ARAM is increased to 415 kW·s more than the BQA and is reduced to 2195 kW·s less than SRMA. The average holding time of ARAM is reduced to 6.25 s less than the BQA and is increased to 37.25 s more than SRMA. The priority loss of ARAM is reduced to 91 less than the BQA and 39 less than SRMA. The operation time of ARMA is the same as that of BQA and SRMA. The traffic flow pressure index is reduced to 0.05 less than the BQA and is increased to 0.45 more than SRMA. The ARAM approach procedure gets the highest score. Therefore, the ARAM approach can also reduce the average holding time of unmanned eVTOL vehicles, decrease the priority loss, and relieve the traffic flow pressure.



(**a**) Holding time boxplot. (**b**) Power consumption boxplot.

Figure 20. Holding time and power consumption comparison boxplot (BQA, ARAM, and AIR).



(**a**) Approach trajectories of BQA. (**b**) Approach trajectories of ARAM.

Figure 21. Approach trajectories (imbalanced traffic flow).

Table 24. Comparison of indexes between BQA, ARAM, and SRMA.

Approach Procedure	F_{total}(*Score*)	*HT*(*Score*)	L_p(*Score*)	*OT*(*Score*)	*P*(*Score*)	*Score*
BQA	*66,300* kW·s *(+2)*	*95* s *(+0)*	*972 (+0)*	*210* s *(+1)*	*0.6 (+0)*	*0.5*
ARAM	*66,715* kW·s *(+1)*	*88.75* s *(+1)*	*881 (+2)*	*210* s *(+0)*	*0.55 (+1)*	*1.7*
SRMA	*68,910* kW·s *(+0)*	*51.5* s *(+2)*	*920 (+1)*	*210* s *(+1)*	*0.1 (+2)*	*1.3*

Tables 25 and 26 display the average power consumption and holding time in different approach priorities. In the ARAM approach procedure, the average power consumption of next-high-priority and high-priority unmanned eVTOL vehicles is reduced to 2018.4 kW·s and 1232.5 kW·s less than the BQA. Its average holding time for middle-priority, next-high-priority, and high-priority unmanned eVTOL vehicles is reduced to 4 s, 71.6 s, and 42.5 s less than the BQA. Its power consumption of middle-priority and high-priority unmanned eVTOLs is reduced to 969 kW·s and 800 kW·s less than SRMA.

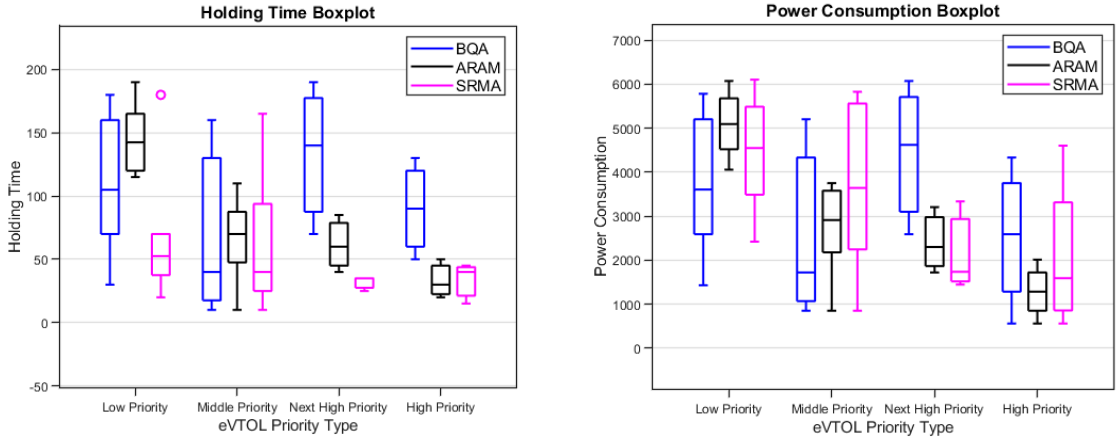
Table 25. Comparison of $\overline{F}$ between BQA, ARAM, and SRMA.

Approach Procedure	Low Priority	Middle Priority	Next High Priority	High Priority
BQA	3750 kW·s	2590 kW·s	4426.7 kW·s	2517.5 kW·s
ARAM	5087.5 kW·s	2730 kW·s	2408.3 kW·s	1285 kW·s
ARMA	4445 kW·s	3699 kW·s	2171.7 kW·s	2085 kW·s

Table 26. Comparison of $\overline{HT}$ between BQA, ARAM, and SRMA.

Approach Procedure	Low Priority	Middle Priority	Next High Priority	High Priority
BQA	110 s	70 s	133.3 s	67.5 s
ARAM	145 s	66 s	61.7 s	25 s
SRMA	65 s	63 s	31.7 s	25 s

The distributions of holding time and power consumption are shown in Figure 22. The power consumption and the holding time of high-priority unmanned eVTOLs in SRMA present a downward concentration distribution compared to the BQA. The holding times of low-priority, middle-priority, and next-high-priority unmanned eVTOL vehicles in ARAM presents an upward dispersion distribution compared to SRMA. The holding time of high-priority unmanned eVTOLs presents a downward distribution compared to SRMA. The power consumption of next-high-priority and high-priority unmanned eVTOL vehicles in ARAM presents a downward concentration distribution compared to the BQA. The power consumption of middle-priority and high-priority unmanned eVTOL vehicles in ARAM presents a downward concentration distribution compared to SRMA.

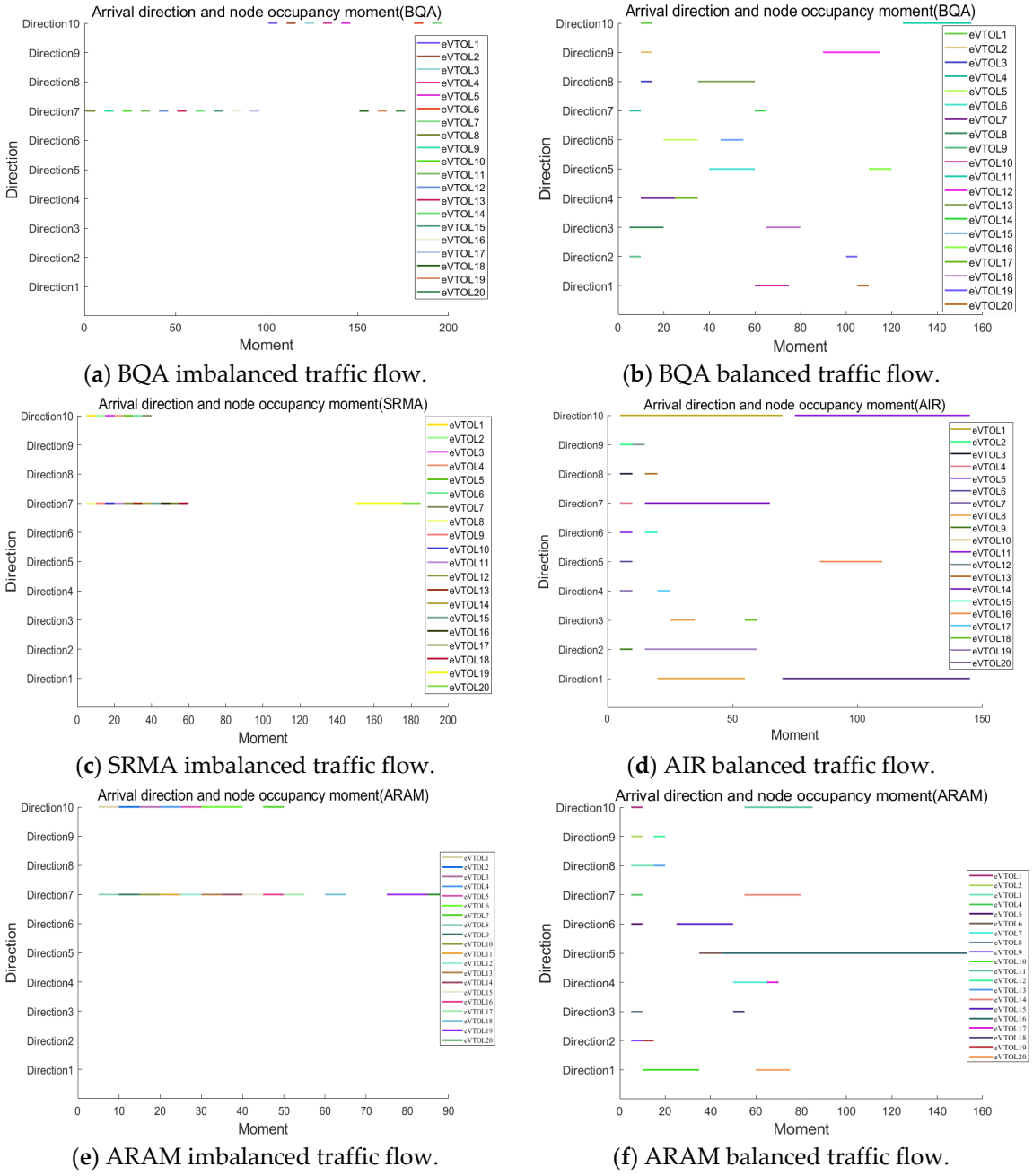


(**a**) Holding time boxplot. (**b**) Power consumption boxplot.

Figure 22. Holding time and power consumption comparison boxplot (BQA, ARAM, and SRMA).

The arrival moment occupancy and arrival direction are shown in Figure 23. It can be concluded that in the scenario of imbalanced traffic flow, the continuity of moment allocation in ARAM and SRMA are better than that of the BQA, which is intermittent. In the scenario of balanced traffic flow, the approach procedures of AIR and ARAM have long occupancy moments, which means these approach procedures are easier to reorder between eVTOLs.

In summary, the ARAM approach procedure can act as an integrated program for unmanned eVTOL approaches in balanced and imbalanced traffic flow scenarios, which can relieve congestion, reduce the holding time, and improve the priority sequencing of unmanned eVTOL vehicles.



(**a**) BQA imbalanced traffic flow.

(**b**) BQA balanced traffic flow.

(**c**) SRMA imbalanced traffic flow.

(**d**) AIR balanced traffic flow.

(**e**) ARAM imbalanced traffic flow.

(**f**) ARAM balanced traffic flow.

Figure 23. Arrival direction and node occupancy moment.

6. Conclusions

This study proposes the AIR approach procedure in a balanced traffic flow scenario, the SRMA approach procedure in an imbalanced traffic flow scenario, and the ARAM approach procedure in a mixed scenario. Furthermore, an unmanned eVTOL priority classification method is proposed to consider unmanned eVTOL flight priority differences. By a computational analysis of typical scenarios, the experimental results are as follows:

(1) The proposed priority loss classification method, direction matrix, and approach procedures can solve the problem of approach sequencing considering unmanned eVTOL flight priority differences and traffic flow imbalance.

(2) In a balanced traffic flow scenario, the ARAM approach procedure has the highest score compared to the BQA and AIR approach procedures. The average holding time of the ARAM approach procedure is reduced to 8.4% and 7.6%, respectively, less

than the BQA and AIR. The ARAM approach procedure is more straightforward for high-priority unmanned eVTOL vehicles in an advanced approach than the BQA.

(3) In an imbalanced traffic flow scenario, the ARAM approach procedure has the highest score compared to the BQA and SRMA approach procedures. Its average holding time is reduced to 6.5% less than the BQA. Its total power consumption has been reduced by 3.1%, less than SRMA. The ARAM approach is more helpful for high-priority unmanned eVTOL vehicles in an advanced approach than the BQA and SRMA in an imbalanced traffic scenario.

The proposed AIR, SRMA, and ARAM approach procedures in this study are used to improve the approach sequencing of unmanned eVTOLs considering unmanned eVTOL flight priority differences. The multi-objective optimization model is constructed to simulate the approach sequencing progress of multiple unmanned eVTOLs. However, the solution time in real-time decision-making is not strong, which is not suitable for larger-scale unmanned eVTOL operations. The factors of uncertainty, departure, and obstacles are not considered in this study. In the future, an optimization algorithm will be designed to accelerate the solution time. The factor of departure will be considered.

Author Contributions: Formal analysis, J.Y.; Resources, Z.W.; Writing—original draft, X.X.; Writing—review & editing, X.X.; Visualization, X.X.; Supervision, X.Z.; Project administration, Z.W. All authors have read and agreed to the published version of the manuscript.

Funding: This research was funded by Tianjin Science and Technology Program Project, grant number 23JCZDJC00580; and National Natural Science Foundation of China, grant number U2133210.

Data Availability Statement: The original contributions presented in this study are included in the article. Further inquiries can be directed to the corresponding author.

Conflicts of Interest: The authors declare no conflict of interest.

References

1. Li, C.; Qu, W.; Li, Y.; Huang, L.; Wei, P. Overview of traffic management of urban air mobility (UAM) with eVTOL aircraft. *J. Traffic Transp. Eng.* **2020**, *20*, 35–54. (In Chinese)
2. Zhang, H.; Zou, Y.; Zhang, Q.; Liu, H. Future urban air mobility management: Review. *Acta Aeronaut. Astronaut. Sin.* **2021**, *42*, 24638. (In Chinese)
3. Hu, Y.; Wang, S.; Zhang, S.; Li, Z. Review of optimization problems, models and methods for airline disruption management from 2010 to 2024. *Digit. Transp. Saf.* **2024**, *3*, 246–263. [CrossRef]
4. Qiu, M.; Le, M.; Hu, Y. Research on Optimal Sequencing of Incoming Flights in Airport Terminal Area. *Aeronaut. Comput. Tech.* **2021**, *222*, 45–49. (In Chinese)
5. Du, Z.; Zhang, J.; Kang, B. A Data-Driven Method for Arrival Sequencing and Scheduling Problem. *Aerospace* **2023**, *10*, 62. [CrossRef]
6. Xu, B.; Ma, W.; Huang, H.; Yue, L. Weighted Constrained Position Shift Model for Aircraft Arrival Sequencing and Scheduling Problem. *Asia-Pac. J. Oper. Res.* **2016**, *33*, 1650028. [CrossRef]
7. Zhang, X.; Zhang, X.; Zhang, J.; Liu, B. Optimization of Sequencing for Aircraft Arrival Based on Approach Routes. In Proceedings of the 2007 IEEE Intelligent Transportation Systems Conference, Bellevue, WA, USA, 30 September–3 October 2007; pp. 592–596.
8. Fulton, N.L.; Wei, P.; Kochenderfer, M.J. Optimal sequencing and scheduling of urban air mobility flights using dynamic programming. *J. Guid. Control. Dyn.* **2018**, *41*, 2085–2096.
9. Benmoussa, A.; Gamboa, P. Effect of Control Parameters on Hybrid Electric Propulsion UAV Performance for Various Flight Conditions: Parametric Study. *Appl. Mech.* **2022**, *4*, 493–513. [CrossRef]
10. Kleinbekman, I.C.; Mitici, M.A.; Wei, P. eVTOL Arrival Sequencing and Scheduling for On-Demand Urban Air Mobility. In Proceedings of the 2018 IEEE/AIAA 37th Digital Avionics Systems Conference (DASC), London, UK, 23–27 September 2018; pp. 1–7.
11. Song, K.; Yeo, H. Development of optimal scheduling strategy and approach control model of multicopter VTOL aircraft for urban air mobility (UAM) operation. *Transp. Res. Part C Emerg. Technol.* **2021**, *128*, 103181. [CrossRef]

12. Song, K.; Yeo, H.; Moon, J.H. Approach Control Concepts and Optimal Vertiport Airspace Design for Urban Air Mobility (UAM) Operation. *Aeronaut. Space Sci.* **2021**, *22*, 982–994. [CrossRef]
13. Hong, Y.; Choi, B.; Lee, S.; Lee, K.; Kim, Y. Optimal and Practical Aircraft Sequencing and Scheduling for Point Merge System. *IFAC-Pap.* **2017**, *50*, 14644–14649. [CrossRef]
14. Errico, A.; Vito, V.D. Study of Point Merge technique for efficient Continuous Descent Operations in TMA. *IFAC-PapersOnLine* **2018**, *51*, 193–199. [CrossRef]
15. Hong, Y.; Choi, B.; Lee, K.; Kim, Y. Dynamic Robust Sequencing and Scheduling Under Uncertainty for the Point Merge System in Terminal Airspace. *IEEE Trans. Intell. Transp. Syst.* **2018**, *19*, 2933–2943. [CrossRef]
16. Liang, M.; Delahaye, D.; Sbihi, M.; Ma, J. Multi-layer Point Merge System for dynamically controlling arrivals on parallel runways. In Proceedings of the 2016 IEEE/AIAA 35th Digital Avionics Systems Conference (DASC), Sacramento, CA, USA, 25–29 September 2016.
17. Tian, Y.; Xing, D.; Ye, B. Study on the Optimization Method of Point Merge Procedure Based on Benefit in the Terminal Area. *Math. Probl. Eng.* **2020**, *2020*, 1–12. [CrossRef]
18. Pradeep, P.; Wei, P. Heuristic Approach for Arrival Sequencing and Scheduling for eVTOL Aircraft in On-Demand Urban Air Mobility. In Proceedings of the 2018 IEEE/AIAA 37th Digital Avionics Systems Conference (DASC), London, UK, 23–27 September 2018.
19. Kleinbekman, I.C.; Mitici, M.; Wei, P. Rolling-Horizon Electric Vertical Takeoff and Landing Arrival Scheduling for On-Demand Urban Air Mobility. *J. Aerosp. Inf. Syst.* **2020**, *17*, 150–159. [CrossRef]
20. Josh, B.; Wei, P. An Efficient Algorithm for Self-Organized Terminal Arrival in Urban Air Mobility. In *AIAA Scitech 2020 Forum*; American Institute of Aeronautics and Astronautics: Reston, VA, USA, 2020.
21. Martin, W.; Okhrin, O.; Schultz, M. Self-organized free-flight arrival for urban air mobility. *Transp. Res. Part C Emerg. Technol.* **2024**, *167*, 104806.
22. Shao, Q.; Shao, M.X.; Lu, Y. Terminal area control rules and eVTOL adaptive scheduling model for multi-vertiport system in urban air Mobility. *Transp. Res. Part C Emerg. Technol.* **2021**, *132*, 103385. [CrossRef]
23. Song, K. Optimal Vertiport Airspace and Approach Control Strategy for Urban Air Mobility (UAM). *Sustainability* **2023**, *15*, 437. [CrossRef]
24. Brunelli, M.; Ditta, C.C.; Postorino, M.N. New infrastructures for Urban Air Mobility systems: A systematic review on vertiport location and capacity. *J. Air Transp. Manag.* **2023**, *112*, 102460. [CrossRef]
25. Xu, Q.; Zhong, Y.; Deng, H.; Wang, X.; Chen, X. Scheduling on tractor and trailer transportation considering the influence of disrupted events based on the contract net and simulated annealing algorithm. *Digit. Transp. Saf.* **2024**, *3*, 155–168. [CrossRef]
26. Ma, J.; Zhang, S.; Wang, M. Effects of dynamic characteristics of lithium-ion battery on flight performance of tilting eVTOL aircraft. *J. Propuls. Technol.* **2024**, *45*, 2211029. (In Chinese)
27. Plett, G. *Battery Management Systems, Volume II: Equivalent-Circuit Methods*; Artech: Norwood, MA, USA, 2015.
28. Sunil, E.; Hoekstra, J.M.; Ellerbroek, J.; Dalmolen, S. Design and evaluation of strategic deconfliction algorithms for UAM operations at vertiports. *Transp. Res. Part C Emerg. Technol.* **2020**, *120*, 102776.
29. Autoflight Prosperity eVTOL. Available online: https://autoflight.com/assets/uploads/files/prosperity-cn.pdf (accessed on 1 March 2025). (In Chinese)
30. Güven, A.; Aybek Cetek, F.; Cecen, R.K. Runway assignment optimisation model for Istanbul Airport considering multiple parallel runway operations. *Aeronaut. J.* **2024**, *128*, 2799–2814. [CrossRef]

Disclaimer/Publisher's Note: The statements, opinions and data contained in all publications are solely those of the individual author(s) and contributor(s) and not of MDPI and/or the editor(s). MDPI and/or the editor(s) disclaim responsibility for any injury to people or property resulting from any ideas, methods, instructions or products referred to in the content.